Kinetic Study of the Copolymerization of Methyl Methacrylate and Methyl Acrylate Using Quantum Chemistry

Xinrui Yu, Seth E. Levine, and Linda J. Broadbelt*

Department of Chemical and Biological Engineering, Northwestern University, Evanston, Illinois 60208-3120

Received June 3, 2008; Revised Manuscript Received August 12, 2008

ABSTRACT: Copolymerization of methyl methacrylate and methyl acrylate was studied using quantum chemistry and transition state theory to estimate the kinetic parameters for propagation (k_p, A, E_a). A terminal model and penultimate effect models were studied explicitly by examining 28 different addition reactions involving monomeric, dimeric, and trimeric radicals and monomers for both self- and cross-propagation. Reactant and product conformations were optimized using a combination of a conventional optimization algorithm and relaxed potential energy scans for individual single-bond rotors using unrestricted B3LYP/6-31G(d). The electronic energy was then calculated using MPWB1K/6-31G(d,p). Low frequencies were treated using a one-dimensional internal rotor model. A and E_a were regressed based on a plot of ln k_p vs $1/T$ over a temperature range of 296.15−800 K. Reactivity ratios (r) characterizing the terminal model were calculated based on the monomeric, dimeric, and trimeric radical addition reactions, and ratios for the explicit penultimate model (r and s) were calculated based on the dimeric and trimeric radical addition reactions and compared to experimental values. The overall propagation rate constant ($k_{p,copo}$) and composition of the copolymer (F) were calculated at different monomer fractions (f). The results based on radical addition of trimeric radicals showed very good agreement with those fitted based on experimental data. Finally, correlation of the activation energies (E_a) with the heats of reactions (ΔH_r) was examined, and the classic Evans−Polanyi relationship was shown to hold well for self- and cross-propagation of methyl acrylates.

1. Introduction

Copolymerization is one of the most commonly used approaches to produce polymers which combine or synergize properties of two or more different parent polymers. For example, the adhesive and cohesive properties of acrylate coating resins can be balanced by controlling the proportions of monomers in the recipe.[1] The kinetics of copolymerization can be quite complicated. In binary copolymerization, there are four different possible combinations of monomers and radical ends, and often the reactivity is influenced by penultimate or further removed units on the propagating radical, further diversifying the number of kinetic parameters that are necessary to capture the composition of the copolymer product. There are no experimental methods capable of directly measuring individual k_p values for different combinations of monomers and radicals. The advent of pulsed laser polymerization in combination with size exclusion chromatography (PLP-SEC) has enabled the determination of the overall propagation rate coefficient ($k_{p,copo}$) for copolymerization systems as well as k_p values for homopolymerization.[2−8] Reactivity ratios relating individual k_p values for homopolymerization and cross-propagation can then be determined based on fitting in the context of a copolymerization model. One such model, the terminal model (TM), classifies the propagating radicals based only on the terminal unit. As depicted in Figure 1, four reaction rate constants (k_{11}, k_{12}, k_{21}, k_{22}) are required to represent all the addition reactions for a binary copolymerization system described according to the terminal model. Two reactivity ratios, r_1 and r_2, are defined as $r_1 = k_{11}/k_{12}$ and $r_2 = k_{22}/k_{21}$ and thus quantify the relative rate of propagation of a radical with its own monomer compared to propagation with the other monomer. Fukuda et al. derived the expression in eq 1 for the overall propagation rate constant ($k_{p,copo}$) as a function of the homopolymerization rate constants of monomer 1 and monomer 2

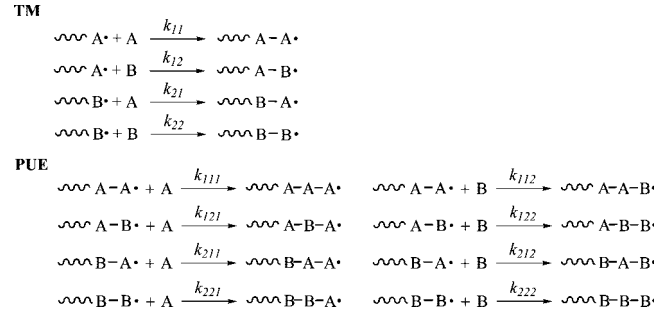

Figure 1. Terminal model (TM) and penultimate effect (PUE) model of binary copolymerization.

(k_{11}, k_{22}), reactivity ratios (r_1 and r_2), and monomer fractions (f_1 and f_2) based on the terminal model.[9] Thus, if $k_{p,copo}$ values are measured at various monomer fractions, the reactivity ratios can be regressed from the equation

$$k_{p,copo} = \frac{r_1 f_1^2 + 2f_1 f_2 + r_2 f_2^2}{(r_1 f_1/k_{11}) + (r_2 f_2/k_{22})} \quad (1)$$

The reactivity ratios can also be regressed from the composition in the copolymer product as a function of monomer fractions as shown in the equation

$$F_1 = \frac{r_1 f_1^2 + f_1 f_2}{r_1 f_1^2 + 2f_1 f_2 + r_2 f_2^2} \quad (2)$$

where F_1 is the fraction of monomer 1 in the copolymer product. Typically, F_i values are measured using spectroscopic methods that are sensitive to the quantity of a specific functional group or structure, such as NMR and near-infrared. However, the reactivity ratios determined using these two methods do not match in some cases. This mismatch has been attributed by

* Corresponding author: phone (847) 491-5351; e-mail broadbelt@northwestern.edu.

10.1021/ma801241p CCC: $40.75
Published on Web 10/08/2008

Fukuda et al. to the neglect of the influence of penultimate units inherent in the assumptions of the TM.[9]

To solve this inconsistency, the penultimate effect (PUE) model was developed.[9] In the PUE model, the reactivity of a radical is dependent on both the terminal and penultimate units. As illustrated in Figure 1, eight reaction rate constants (k_{hij}, h, i, $j = 1, 2$) are required to cover all the addition reactions for a binary copolymerization system. Four reactivity ratios (r_{ij}) and two radical reactivity ratios (s_i) are introduced as follows:

$$r_{11} = \frac{k_{111}}{k_{112}}, \quad r_{12} = \frac{k_{122}}{k_{121}}, \quad r_{22} = \frac{k_{222}}{k_{221}}, \quad r_{21} = \frac{k_{211}}{k_{212}}, \quad s_1 = \frac{k_{211}}{k_{111}}, \quad s_2 = \frac{k_{122}}{k_{222}}$$

The overall propagation rate coefficient ($k_{p,copo}$) is then expressed based on the homopolymerization rate constants and reactivity ratios as in the equation

$$k_{p,copo} = \frac{\bar{r}_1 f_1^2 + 2f_1 f_2 + \bar{r}_2 f_2^2}{(\bar{r}_1 f_1/\bar{k}_{11}) + (\bar{r}_2 f_2/\bar{k}_{22})} \tag{3}$$

where the average reactivity ratios ($\bar{r}_1$ and $\bar{r}_2$) and rate coefficients ($\bar{k}_{ii}$) are defined as in the equation

$$\bar{r}_i = r_{ji}\frac{r_{ii}f_i + f_j}{r_{ji}f_i + f_j} \qquad \bar{k}_{ii} = k_{iii}\frac{r_{ii}f_i + f_j}{r_{ii}f_i + f_j/s_i} \tag{4}$$

The composition of each monomer in the copolymer (F_i) is then written based on the average reactivity ratios defined in eq 4 as in the equation

$$F_1 = \frac{\bar{r}_1 f_1^2 + f_1 f_2}{\bar{r}_1 f_1^2 + 2f_1 f_2 + \bar{r}_2 f_2^2} \tag{5}$$

The PUE model including six ratios (r_{11}, r_{12}, r_{21}, r_{22}, s_1, and s_2) is called the explicit penultimate effect (EPUE) model. If it is assumed that the reactivity ratios of different penultimate units are close, i.e., $r_{11} \approx r_{21} = r_1$ and $r_{22} \approx r_{12} = r_2$, the implicit penultimate effect (IPUE) model is obtained, which uses four ratios (r_1, r_2, s_1, and s_2) to describe the overall propagation rate coefficient and copolymer composition.

While both the TM and PUE models have been widely used to study copolymerization and quantify the governing parameters, neither of these two methods can be used to determine the kinetic parameters (E_a and A) for the individual reactions directly. In addition, determination of the kinetic parameters indirectly by assuming a model can be confounded by other reactions taking place at the reaction conditions necessary to extract meaningful E_a and A values. For example, in PLP-SEC, secondary reactions like transfer reactions need to be suppressed, so the PLP-SEC experiments are carried out at low temperatures.[10,11] Thus, it may not be possible to measure the parameters of interest over a wide temperature range. Therefore, it is attractive to have a methodology to determine all of the kinetic parameters governing copolymerization directly in the absence of any competing reactions. The ability to predict kinetic parameters would enable modeling of copolymerization processes and offer guidance for the development of novel monomers.

In previous research, we developed a methodology based on quantum chemistry and transition state theory to calculate kinetic parameters for the homopolymerization of methyl methacrylate and methyl acrylate.[12] We demonstrated that k_p values in excellent agreement with experiment could be calculated based on ab initio calculations. In the present work, the same methodology was used to calculate the kinetic parameters for the copolymerization of methyl methacrylate and methyl acrylate. Terminal model and penultimate model kinetic parameters were obtained by varying the radical reactants, and the results were compared to experimental data.

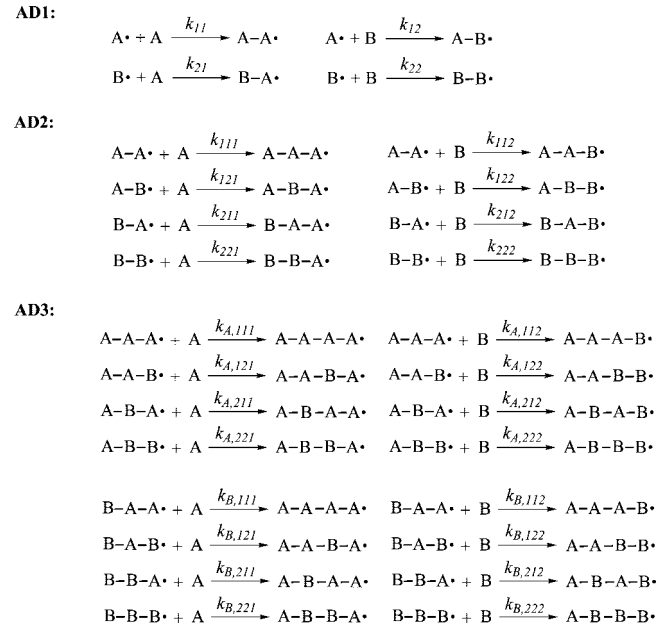

Figure 2. Addition reactions of monomeric, dimeric, and trimeric radicals to monomers in methyl methacrylate−methyl acrylate copolymerization. "A" stands for methyl methacrylate and "B" stands for methyl acrylate; ADn is used to denote an addition reaction involving a radical reactant of length n.

In addition, the ability to calculate individual rate parameters for self- and cross-propagation reactions explicitly allowed the applicability of different descriptions of radical reactivity to be tested for acrylates. A number of researchers have investigated the ability of simple structure−reactivity relationships to capture reactivity trends in radical reactions.[13−15] In particular, the Evans−Polanyi relationship, in which the activation energy (E_a) and heat of reaction (ΔH_r) are linearly correlated as shown in eq 6, has been tested.

$$E_a = E_0 + \alpha \Delta H_r \tag{6}$$

The coefficients E_0 and α are constant for reactions in the same family. The Evans−Polanyi relationship is an empirical description which only includes the influence of enthalpic factors on the activation energy. It has been shown that there are additional factors influencing the activation energy such as polar and steric effects.[13] In order to investigate the factors that influence the activation energy fully, a more detailed analysis, such as that provided by a state correlation diagram (SCD),[16,17] is warranted. Nevertheless, the Evans−Polanyi relationship is still widely used to estimate activation energies because of its simplicity and its ability to capture a large portion of the variation of E_a values with structure. The detailed calculations performed here offer the opportunity to test the Evans−Polanyi relationship and its utility in estimating reactivity ratios based on enthalpic differences alone.

2. Computational Methodology

Twenty-eight addition reactions of monomeric, dimeric, and trimeric radicals to monomers in all possible different combinations were studied for methyl methacrylate−methyl acrylate copolymerization as shown in Figure 2, in which "A" stands for methyl methacrylate and "B" denotes methyl acrylate. On

the basis of the number of units in the radical, the reactions are divided into three groups: AD1, AD2, and AD3, where AD*n* denotes an addition reaction involving a radical reactant of length *n*.

The AD1 set includes four reactions, which are used to simulate the terminal model only. The AD2 set includes eight reactions, which are used to simulate both the penultimate model and the terminal model, if the reactivity ratios are calculated as the average values of those for radicals with the same end unit but different penultimate units. To explore the influence of the penpenultimate unit, an additional methyl methacrylate or methyl acrylate unit was added to the eight AD2 radicals to construct 16 AD3 reactions, from which the TM and PUE parameters were calculated based on average ratios. For all reactions, the kinetic parameters (k_p, A, and E_a) were calculated individually. The heats of reactions (ΔH_r) for these reactions were also calculated to assess the applicability of the Evans−Polanyi equation.

All electronic energy calculations and vibrational frequencies were calculated using Gaussian 03.[18] All the reactant and product conformations were optimized using unrestricted B3LYP/6-31G(d) first via conventional optimization. However, the conventional optimization method employed is based on the gradient in energy and can only locate local minima,[19] and thus the optimized geometry is sensitive to the input structure. Therefore, a combination of conventional optimization and relaxed potential energy scans for all the single bond dihedrals was used. This method is based on the fact that different conformations are mainly due to variations in the rotation about single bonds. Specifically, one-dimensional relaxed potential energy scans were carried out with the keyword "modredundant" with 30° as the scan interval. If a lower energy structure was detected, it was optimized conventionally, and the process was repeated until no conformations of lower energy were obtained. The detailed method and comparison of different levels of theory and scan intervals for performing the one-dimensional scans have been discussed previously.[12,20]

Transition state structures were identified using the QST3 method, which requires the reactants, product, and an estimated transition state (TS) conformation as input.[21] On the basis of our experience with homopolymerization, the initial guesses for the TS conformations were constructed by elongating the product carbon−carbon bond to 2.3 Å. Transition states were confirmed to have one imaginary frequency, which corresponded to the motion along the reaction coordinate, and an intrinsic reaction coordinate (IRC) following with a step size of 0.1 amu$^{0.5}$ bohr was used to verify that the correct reactants and product were obtained.

Because of the size of the species studied here, it is critical to have a quantum chemical calculation method/basis set which is accurate yet computationally affordable. Various hybrid density functional theory (DFT) methods and basis sets were compared in our previous research for the homopolymerization of methyl methacrylate and methyl acrylate.[12] It was found that the modified Perdew−Wang and Becke functional (MPWB1K) with the basis set of 6-31G(d,p) provided activation energies and k_p values which are in very good agreement with experimental data. Therefore, MPWB1K/6-31G(d,p) was also used to calculate the electronic energy for the copolymerization reactions. The zero-point vibrational energy (ZPVE) was calculated using UB3LYP/6-31G(d) with a scale factor of 0.9806.[22] A scale factor of 1.0002 was used in the calculation of partition functions based on the recommended scale factors for ΔH_{vib} and ΔS_{vib} reported by Scott and Radom.[22]

The reaction rate constant at a specific temperature was calculated using eq 7:[14]

$$k(T) = \kappa(T)\frac{k_B T}{h}(c^\circ)^{1-m}\frac{Q^{\ddagger}}{Q_{mon}Q_{rad}}e^{-\Delta E_0/RT} \quad (7)$$

in which $k(T)$ is the tunneling factor, which deviates from a value of one for reactions involving motion of light atoms such as hydrogen transfer, but can be set equal to one for propagation reactions of acrylates. k_B is Boltzmann's constant (1.3806×10^{-23} J mol^{-1} K^{-1}), h is Planck's constant (6.6261×10^{-34} J s), m is the number of reactants, which is two for propagation, c° is the standard state concentration (mol L^{-1}) to which the quantum chemical calculations are referenced, P/RT, where P is 1 atm, and ΔE_0 is the difference between E_0 of the transition state and the reactants, which is defined as the summation of the electronic energy (E_e) and the zero-point vibrational energy (ZPVE). The ZPVE is the contribution to the energy from vibration at 0 K as defined in eq 8.[23]

$$\mathrm{ZPEV} = \frac{1}{2}\sum_i^{3N-6} h\nu_i \quad (8)$$

in which N is the number of atoms and ν_i represents the frequencies. The final quantity in eq 7 is the partition function (Q), which is conventionally written as the product of different modes as shown in eq 9.[23]

$$Q = Q_e Q_{tr} Q_r Q_v \quad (9)$$

where Q_e is the electronic partition function, which is one for the ground state, Q_{tr} accounts for the translational motion, and Q_r is for the species' rotational motion as a whole. The remaining motions are captured by Q_v, which is typically calculated using a harmonic oscillator model. However, the harmonic oscillator model is not an accurate description of all of these motions, especially those associated with low frequencies, which are mainly composed of rotational motions. The importance of treating low frequencies using a more suitable model has been realized and applied in recent research.[14,24−31] In our methodology, all the frequencies and corresponding vibrational partition functions (Q_v) were calculated using UB3LYP/6-31G(d). The low frequencies were then separated from the harmonic oscillator partition function and treated using a one-dimensional internal rotor model. Thus, the partition function written in eq 9 is revised as eq 10.

$$Q = Q_e Q_{tr} Q_r Q_{vib} Q_{int,rot} \quad (10)$$

where $Q_{int,rot}$ is the contribution from those vibrations better treated as internal rotations. To obtain $Q_{int,rot}$, all the single bonds were treated as rotation axes. For transition states, the bond defining the transition state was also treated as a rotation axis since it was found that the lowest positive frequency mainly consists of the torsional motion about the bond defining the transition state. As an example, the nine internal rotors in the transition state for addition of methyl methacrylate monomeric radical to monomer are shown in Figure 3. For the mth rotation, the partition function was calculated based on the definition of the partition function as shown in eq 11.

$$Q_{int,rot,m} = \frac{1}{\sigma_m}\sum_i \exp\left(-\frac{\epsilon_i}{k_B T}\right) \quad (11)$$

in which σ_m is the symmetry number of the mth internal rotor and ϵ_i are the energy levels calculated by solving the one-dimensional Schrödinger equation shown in eq 12:

$$-\frac{\hbar^2}{2I_{red}}\frac{d^2}{d\theta^2}\Psi + V(\theta)\Psi = \epsilon\Psi \quad (12)$$

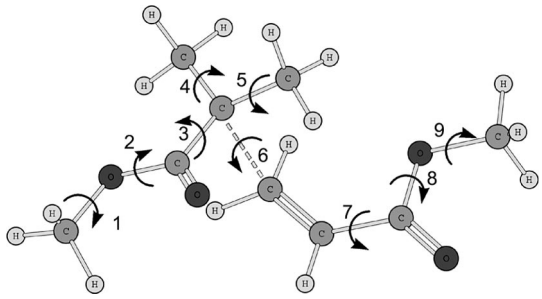

Figure 3. Internal rotations about all eight single bonds and the bond defining the transition state for the transition state of the methyl methacrylate AD1 (Figure 2) reaction were considered.

where $\hbar$ is Planck's constant divided by 2π, Ψ is the wave function, and θ is the rotation angle. I_{red} is the reduced moment of inertia (I_{red}^2 defined by East et al.[32]). $V(\theta)$ is the potential energy expressed as a function of torsional angle, which is in the form of a full Fourier expansion as shown in eq 13.

$$V(\theta) = \sum_{i=1}^{n} [a_i(1 - \cos i\theta) + b_i \sin i\theta] \tag{13}$$

Equation 13 can be expressed in the form of a matrix product, and the coefficients a_i and b_i are then determined by solving an overdetermined function. It has been verified that energy scans with 12 sampling points and $n = 3$ in eq 13 are sufficient to capture both symmetric and asymmetric energy profiles.[12] The one-dimensional Schrödinger equation was solved with the Fourier grid Hamiltonian (FGH) method, in which the Hamiltonian operator was expressed in the form of a matrix and the energy levels were determined by diagonalizing the matrix.[33] In the construction of the Hamiltonian operator matrix, the rotation range from 0 to 360° was discretized using 1000 grid points, which was verified to have partition functions in agreement with those from finer grid sizes.[12,20] For the partition functions of the low frequencies which should be substituted by those calculated based on the internal rotor model, there is no well accepted cutoff value to define "low" frequencies. 200 cm^{-1} was used as the upper limit to define low frequencies in some research,[24] while 300 cm^{-1} was used by other researchers.[25] In these cases, the frequencies lower than the cutoff value were taken out of Q_v and replaced by $Q_{int,rot}$, which is the product of the internal rotor partition functions for each rotor. For very simple molecules like ethane, 99% of the lowest frequency corresponds to the rotation about the carbon−carbon single bond which can be ascertained from analysis of the normal modes. The frequency corresponding to a rotor for such simple molecules can be visually confirmed by animating the vibrational modes. However, these methods are not suitable for complex molecules like methyl methacrylate since each frequency is a mixture of multiple modes. In this research, we did not apply an arbitrary upper limit to define low frequencies. Instead, the number of low frequencies (excluding the imaginary frequency in the transition state) which were removed from Q_v was set equal to the number of rotors, which included rotations about σ bonds and the bond forming in the transition state. Rather than simply removing the contribution of the N lowest frequencies from Q_{vib}, where N is the number of rotors, the low frequencies were examined to be sure they consisted of rotational components.

The activation energy (E_a) and frequency factor (A) were determined from the regression of ln $k_p(T)$ vs $1/T$ over the temperature range of 296.15−800 K in 50 K intervals, according to eq 14.

$$\ln k_p(T) = \ln A - \frac{E_a}{RT} \tag{14}$$

Monomer reactivity and radical reactivity ratios were calculated based on k_p values, and the $k_{p\,copo}$ and F_i values were calculated using the expressions presented above for the TM and PUE models. The calculated ratios, $k_{p,copo}$, and F_i values were compared to experimental data regressed or measured at 23 °C and 1000 bar by Buback et al.[34] In order to be able to compare the calculated values to those of Buback and coworkers at 1000 bar, the results from the quantum chemistry calculations, which are at ambient pressure, were adjusted using the activation volume ($V^{\ddagger}$) as shown in eq 15.[35]

$$\frac{d \ln k_p}{dp} = -\frac{\Delta V^{\ddagger}}{RT} \tag{15}$$

The activation volume ($V^{\ddagger}$) for methyl methacrylate is −16.7 $cm^3\ mol^{-1}$ and for methyl acrylate is −11.7 $cm^3\ mol^{-1}$.[11,36] No activation volume value for a methyl methacrylate and methyl acrylate copolymerization system is reported, so the average value of the two monomers of −14.2 $cm^3\ mol^{-1}$ was used. The ratios of the rate coefficients between ambient pressure and 1000 bar at various temperatures based on these activation volumes are listed in Table 1. At 23 °C, the ratios are 2.0 for methyl methacrylate, 1.6 for methyl acrylate, and 1.8 for the mixture of methyl methacrylate and methyl acrylate. Note that our assumption of an average value for the copolymer system based on the two monomeric components and the relatively close values of $V^{\ddagger}$ for methyl methacrylate and methyl acrylate will lead to reactivity ratios that are nearly independent of pressure.

The following reactivity ratios and rate coefficients for methyl methacrylate−methyl acrylate copolymerization at 23 °C and 1000 bar provided by Buback et al. were used for comparison.[34]

- Reactivity ratios based on TM fitted from composition plot: $r_1 = 3.03$, $r_2 = 0.20$.
- Reactivity ratios based on TM fitted from $k_{p,copo}$ measured using PLP-SEC: $r_1 = 1.95$, $r_2 = 0.21$.
- Monomer reactivity and radical reactivity ratios based on IPUE model fitted from $k_{p,copo}$ measured using PLP-SEC: $r_1 = 2.40$, $r_2 = 0.18$, $s_1 = 1.46$, $s_2 = 0.38$.
- Homopolymerization propagation rate coefficients of methyl methacrylate and methyl acrylate at 23 °C and 1000 bar: $k_{p,MMA} = 702$ L $mol^{-1}\ s^{-1}$, $k_{p,MA} = 18\,088$ L $mol^{-1}\ s^{-1}$.

3. Results and Discussion

3.1. Geometries and Transition States. Interesting features related to the reactivity of the different radical and monomer combinations were apparent from the geometries of the transition states. For example, the conformations of the four AD1 reactions are shown in Figure 4. Comparison of all of the transition states shows that for the same radical the bond length defining the transition state formed by the radical and methyl acrylate is about 0.01 Å shorter than that in the transition state structure formed with methyl methacrylate, which reveals that the transition states involving methyl methacrylate monomer are located earlier along the reaction coordinate. The bond lengths defining the transition state of addition of radicals to methyl methacrylate vary from 2.239 to 2.313 Å, while those for addition to methyl acrylate vary from 2.222 to 2.302 Å. An earlier transition state translates into a lower activation energy and higher reaction exothermicity, which is consistent with the calculated activation energies and heats of reaction reported below.

3.2. Kinetics. The activation energies and frequency factors of the four reactions involving the addition of monomeric radical to monomer (AD1) are listed in Table 2. It can be seen that for

Table 1. Ratios of Propagation Rate Coefficients at 1000 bar to Those at Ambient Pressure Calculated Using Eq 15 over the Temperature Range of 296.15−476.15 K[a]

temp (K)	$k_{p,1000\ bar}/k_{p,1\ atm}$ (MMA)	$k_{p,1000\ bar}/k_{p,1\ atm}$ (MMA/MA)	$k_{p,1000\ bar}/k_{p,1\ atm}$ (MA)
296.15	2.0	1.8	1.6
326.15	1.9	1.7	1.5
356.15	1.8	1.6	1.5
386.15	1.7	1.6	1.4
416.15	1.6	1.5	1.4
446.15	1.6	1.5	1.4
476.15	1.5	1.4	1.3

[a] Activation volume for methyl methacrylate: -16.7 cm^3 mol^{-1}; activation volume for methyl acrylate: -11.7 cm^3 mol^{-1}; activation volume for a methyl methacrylate and methyl acrylate copolymer system is calculated as the average of the two monomers: -14.2 cm^3 mol^{-1}.

both methyl methacrylate and methyl acrylate monomeric radicals the activation energies for the addition to methyl methacrylate monomer are lower than the corresponding ones for the addition to methyl acrylate monomer. The difference for methyl methacrylate radical is about 7 kJ mol^{-1}, while that for methyl acrylate radical is about 4 kJ mol^{-1}. This is consistent with simple radical stability arguments and indicates that the activation energy is dominated by enthaplic effects. Addition to methyl methacrylate monomer involves the formation of a more stable tertiary radical, compared to the formation of a secondary radical in the case of methyl acrylate monomer. Thus, addition to methyl methacrylate monomer is enthalpically preferred. This preference also manifests itself in the reaction exothermicity: methyl methacrylate radical reacting with methyl methacrylate monomer is 1.3 kJ mol^{-1} more exothermic than addition to methyl acrylate monomer, while for methyl acrylate radical, reaction with methyl methacrylate is 6.3 kJ mol^{-1} more exothermic than addition to methyl acrylate. However, addition to the less bulky methyl acrylate is entropically preferred. For the same radical, reaction with methyl acrylate monomer has a higher frequency factor such that $A_{11}/A_{12} = 0.28$ and $A_{21}/A_{22} = 0.24$. The calculated homopolymerization rate constants ($k_{11} = 9.53 \times 10^1$ L mol^{-1} s^{-1}, $k_{22} = 2.57 \times 10^3$ L mol^{-1} s^{-1}) are 13% and 14% of the measured homopolymerization rate constants of methyl methacrylate and methyl acrylate ($k_{p,MMA} = 7.02 \times 10^2$ L mol^{-1} s^{-1}, $k_{p,MA} = 1.81 \times 10^4$ L mol^{-1} s^{-1}), respectively. These results at higher pressure are consistent with our previous results at atmospheric pressure, where we recommended using trimeric radicals at a minimum to achieve results that were in excellent quantitative agreement with experiment.[12] Nonetheless, the AD1 results still capture the reactivity trends observed in the experimental values.

It is next interesting to evaluate the reactivity ratios predicted from the AD1 reactions, i.e., the terminal model. These are tabulated in Table 3 as a function of temperature. Buback et al. determined reactivity ratios based on the terminal model at 23 °C and 1000 bar from two different types of experimental data: (1) polymer composition (Mayo−Lewis plot): $r_1 = 3.03$, $r_2 = 0.20$; (2) the overall propagation rate constant $k_{p,copo}$ measured using PLP-SEC: $r_1 = 1.95$, $r_2 = 0.21$. The ratios determined based on the calculated kinetic parameters at the same conditions are $r_1 = 5.14$ and $r_2 = 0.77$. While these quantities have the same trend, i.e., k_{11} is higher than k_{12} and k_{22} is lower than k_{21}, they are not in perfect quantitative agreement. This is consistent with our previous assertion that monomeric radicals are simply too small to capture polymeric reactions quantitatively.

The results for the dimeric radical addition reactions (AD2) are tabulated in Table 4. The activation energies (E_a) and frequency factors (A) of the eight AD2 reactions in Figure 2 are listed. The reactivities of methyl methacrylate and methyl acrylate have the same tendencies as were observed for the AD1 results; i.e., reaction of radicals with methyl methacrylate monomer is enthalpically favored as reflected by lower activation energies (0.9−3.1 kJ mol^{-1} lower) and more exothermic heats of reaction (4.1−7.6 kJ mol^{-1} more exothermic). The ratios of the frequency factors are $A_{111}/A_{112} = 1.58$, $A_{121}/A_{122} = 0.66$, $A_{211}/A_{212} = 0.58$, and $A_{221}/A_{222} = 0.35$. In general, addition to methyl acrylate is slightly favored entropically. The calculated propagation rate constants of methyl methacrylate (1.68×10^2 L mol s^{-1}) and methyl acrylate (9.65×10^3 L mol s^{-1}) at 23 °C and 1000 bar are closer to the measured data ($k_{p,MMA} = 7.02 \times 10^2$ L mol^{-1} s^{-1}, $k_{p,MA} = 1.81 \times 10^4$ L mol^{-1} s^{-1}) than those obtained using the AD1 model. However, they are not as close as those obtained in our earlier work for the addition of trimeric radicals.

Reactivity ratios characterizing the terminal model were calculated based on the AD2 reactions as listed in Table 5. Two different r_1 and two different r_2 values were calculated from the eight reactions, where a given r_i value had the same penultimate unit for the radicals. It is clear that the calculated r_i values based on different penultimate units are not consistent. For example, the two r_2 values calculated based on the AB$^\bullet$ and BB$^\bullet$ radicals are opposite at 23 °C: $k_{122}/k_{121} < 1$ while $k_{222}/k_{221} > 1$. The two r_1 values are both greater than one, but the values are not close ($k_{111}/k_{112} = 6.17$, $k_{211}/k_{212} = 1.99$). Thus, there are two possibilities: terminal model kinetics are not a good description of this copolymerization system, or dimeric radicals are not sufficient to capture the correct penultimate unit effects. To explore the latter possibility, monomer and radical reactivity ratios for the EPUE model were also calculated based on these AD2 reactions as listed in Table 6 over a range of temperatures and at 1000 bar. At the experimental conditions (23 °C, 1000 bar), the calculated reactivity ratios ($r_{11} = 6.17$, $r_{21} = 1.99$, $r_{22} = 1.67$, $r_{21} = 1.99$) and radical ratios ($s_1 = 0.91$, $s_2 = 0.33$) have noticeable deviation from those determined from PLP-SEC measurements using the IPUE model: $r_1 = 2.40$, $r_2 = 0.18$, $s_1 = 1.46$, $s_1 = 0.38$. This reinforces our earlier contention based on homopolymerization studies that using addition of dimeric radicals is not sufficient to predict reactivity measurements in polymeric systems.

Therefore, we further extended the chain length of the radicals studied and investigated the reaction of trimeric radicals (AD3 in Figure 2). Two different groups of radicals were studied: radicals with methyl methacrylate (A) as the penpenultimate unit (A-AD3) and radicals with methyl acrylate (B) as the penpenultimate unit (B-AD3). This provided both a more realistic mimic of polymeric reactions while also allowing the investigation of penpenultimate unit effects. The activation energies and frequency factors of the eight A-AD3 reactions and the eight B-AD3 reactions are listed in Table 7. Addition to the methyl methacrylate monomer is still enthalpically preferred as reflected in the lower activation energies (2.6−3.4 kJ mol^{-1} lower) and more exothermic heats of reaction (5.7−9.4 kJ mol^{-1} more exothermic). The ratios of the frequency factors when A is the penpenultimate unit are $A_{A,111}/A_{A,112} = 0.72$, $A_{A,121}/A_{A,122} = 0.64$, $A_{A,211}/A_{A,212} = 0.77$, and $A_{A,221}/A_{A,222} = 0.76$, which indicates that the addition to methyl acrylate is entropically favored. The calculated propagation rate coefficient for methyl methacrylate homopolymerization is 3.02×10^2 L mol^{-1} s^{-1} and 1.69×10^3 L mol^{-1} s^{-1} for methyl acrylate. The A-AD3 rate coefficient for methyl methacrylate is close to the experimental value (7.02×10^2 L mol^{-1} s^{-1}) while the A-AD3 rate coefficient for methyl acrylate is about 1 order of magnitude lower than the experimental methyl acrylate homopolymerization rate coefficient (1.84×10^4 L mol^{-1} s^{-1}). For the eight AD3 reactions with methyl acrylate as the penpenultimate unit (B-AD3) in Figure 2, it can be seen that addition to methyl methacrylate is still enthalpically preferred as reflected in the lower activation energies (2.9−6.1 kJ mol^{-1} lower) and more

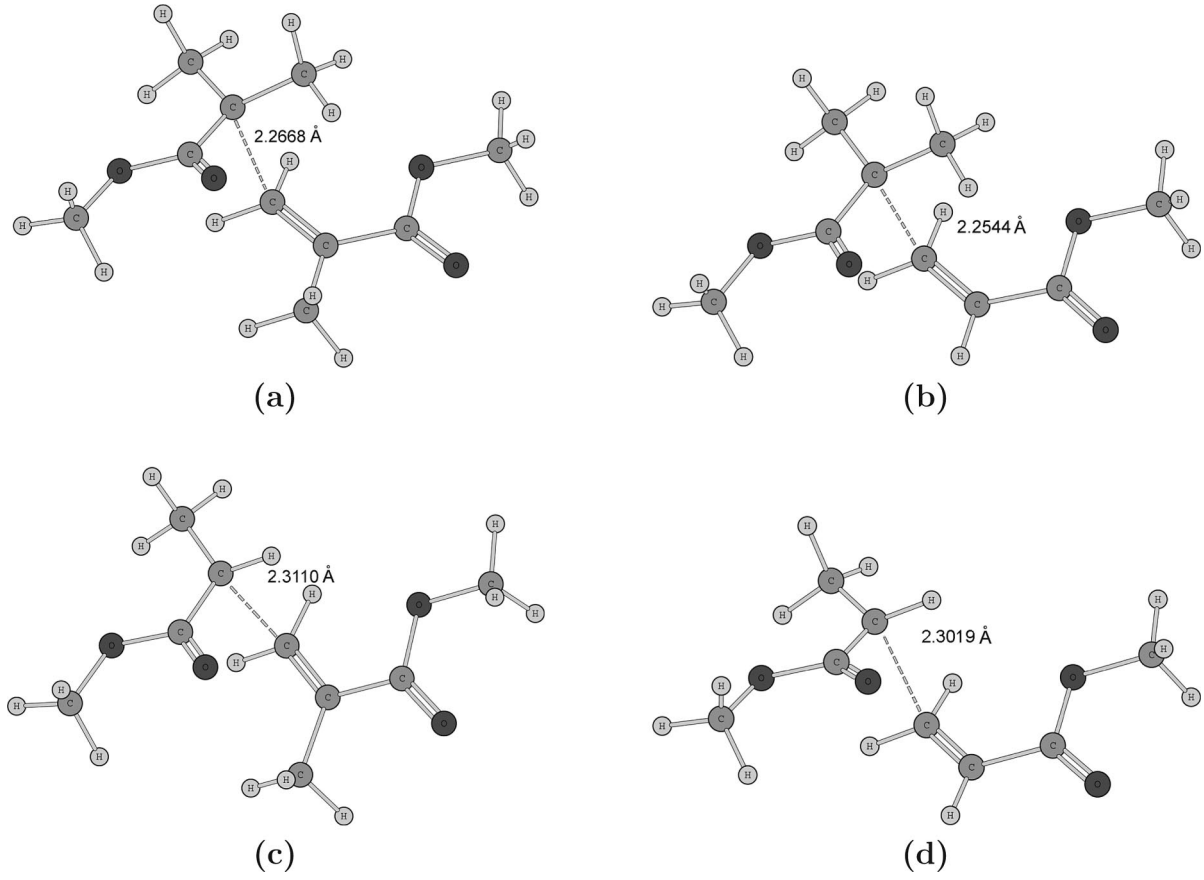

Figure 4. Structures and bond lengths of transition states for the four methyl methacrylate−methyl acrylate AD1 copolymerization reactions summarized in Figure 2: (a) methyl methacrylate radical−methyl methacrylate monomer; (b) methyl methacrylate radical−methyl acrylate monomer; (c) methyl acrylate radical−methyl methacrylate monomer; (d) methyl acrylate radical−methyl acrylate monomer.

Table 2. Activation energies (E_a), Frequency Factors (A), Heats of Reaction (ΔH_r), and Rate Constants (k_p at 23 °C, 1000 bar) for the Methyl Methacrylate−Methyl Acrylate AD1 (TM) Reactions[a]

reactions		E_a	A	ΔH_r (23 °C)	k_p (23 °C, 1000 bar)
$A^{\bullet} + A \rightarrow AA^{\bullet}$	k_{11}	27.7	3.72×10^6	−50.1	9.53×10^1
$A^{\bullet} + B \rightarrow AB^{\bullet}$	k_{12}	34.6	1.32×10^7	−48.8	1.85×10^1
$B^{\bullet} + A \rightarrow BA^{\bullet}$	k_{21}	22.5	1.74×10^7	−76.5	3.33×10^3
$B^{\bullet} + B \rightarrow BB^{\bullet}$	k_{22}	26.4	7.24×10^7	−70.2	2.57×10^3

[a] Geometry optimization and frequency calculations were performed using UB3LYP/6-31G(d), electronic energies were calculated using MPWB1K/6-31G(d,p), and low frequencies were treated using a one-dimensional internal rotor model A: methyl methacrylate, B: methyl acrylate; rate coefficients were first calculated at ambient pressure and adjusted to 1000 bar using the factors listed in Table 1 (k_p: L mol^{-1} s^{-1}, E_a: kJ mol^{-1}, A: L mol^{-1} s^{-1}, ΔH_r: kJ mol^{-1}).

exothermic heats of reaction (4.2−14.8 kJ mol^{-1} more exothermic). Methyl acrylate is entropically preferred as reflected in the higher frequency factors. The ratios of the frequency factors are $A_{B,111}/A_{B,112} = 0.87$, $A_{B,121}/A_{B,122} = 0.81$, $A_{B,211}/A_{B,212} = 0.72$, and $A_{B,221}/A_{B,222} = 0.21$. The calculated propagation rate coefficients for methyl methacrylate homopolymerization (3.85×10^2 L mol^{-1} s^{-1}) and methyl acrylate (1.56×10^4 L mol^{-1} s^{-1}) at 23 °C and 1000 bar are in very good agreement with the experimental data ($k_{p,MMA} = 7.02 \times 10^2$ L mol^{-1} s^{-1}, $k_{p,MA} = 1.81 \times 10^4$ L mol^{-1} s^{-1}). The better agreement of the rate coefficient for methyl acrylate homopolymerization for the B-AD3 reaction suggests that the penpenultimate unit still has an influence on the absolute rate coefficient values for methyl acrylate, while the influence of the penpenultimate unit for methyl methacrylate is less pronounced.

Table 3. Calculated TM Reactivity Ratios (r_1, r_2) for Methyl Methacrylate−Methyl Acrylate Copolymerization Based on the Four AD1 Reactions in Figure 2 over the Temperature Range of 296.15−476.15 K and at 1000 bar and Reactivity Ratios Fitted from Experimental Data at 296.15 K Based on TM by Buback et al.[34] [a]

T (K)	r_1	r_2
296.15	5.14	0.77
326.15	3.94	0.90
356.15	3.15	1.02
386.15	2.61	1.14
416.15	2.23	1.25
446.15	1.94	1.36
476.15	1.72	1.46
fitted from composition plot	3.03	0.20
fitted from $k_{p,copo}$ (PLP-SEC)	1.95	0.21

[a] Kinetic parameters are listed in Table 2, and the pressure adjustment ratios are listed in Table 1.

The calculated TM ratios based on the AD3 reactions are listed in Table 8. The r_i values were calculated for reactions that had the same penpenultimate and penultimate units; thus, four r_1 values and four r_2 values were calculated based on the 16 reactions. The calculated ratios for different penpenultimate and penultimate units are extremely consistent: at 23 °C, the four r_1 values are 2.50, 3.08, 3.11, and 3.25; the four r_2 values are 0.38, 0.38, 0.38, and 0.36. The AD3 reactions also allow monomer and radical reactivity ratios for the explicit PUE model to be calculated as listed in Table 9 over a range of temperatures and at 1000 bar. Note that the r_{ij} values in Table 9 are the same as the r_i values reported in Table 8 but are repeated in Table 9 with their more specific r_{ij} designation that characterizes the EPUE model. The results from the trimeric radical addition reactions capture the experimental PUE reactivity ratios very

Table 4. Activation Energies (E_a), Frequency Factors (A), Heats of Reaction (ΔH_r), and Rate Constants (k_p at 23 °C, 1000 bar) for the Methyl Methacrylate−Methyl Acrylate AD2 (PUE) Reactions[a]

reactions		E_a	A	ΔH_r (23 °C)	k_p (23 °C, 1000 bar)
AA• + A → AAA•	k_{111}	28.0	7.41×10^6	−41.2	1.68×10^2
AA • + B → AAB•	k_{112}	31.1	4.68×10^6	−37.1	2.72×10^1
A• + A → ABA•	k_{121}	19.0	8.91×10^6	−75.2	7.00×10^3
AB• + B → ABB•	k_{122}	22.0	1.35×10^7	−68.0	3.19×10^3
BA• + A → BAA•	k_{211}	26.8	4.47×10^6	−47.5	1.52×10^2
BA• + B → BAB•	k_{212}	29.8	7.76×10^6	−42.8	7.65×10^1
BB• + A → BBA•	k_{221}	21.7	2.19×10^7	−78.4	5.80×10^3
BB • + B → BBB•	k_{222}	22.8	6.31×10^7	−70.8	9.65×10^3

[a] Geometry optimization and frequency calculations were performed using UB3LYP/6-31G(d), electronic energies were calculated using MPWB1K/6-31G(d,p), and low frequencies were treated using a one-dimensional internal rotor model A: methyl methacrylate, B: methyl acrylate; rate coefficients were first calculated at ambient pressure and adjusted to 1000 bar using the factors listed in Table 1. (k_p: L mol^{-1} s^{-1}, E_a: kJ mol^{-1}, A: L mol^{-1} s^{-1}, ΔH_r: kJ mol^{-1}).

Table 5. Calculated TM Reactivity Ratios (r_1, r_2) for Methyl Methacrylate−Methyl Acrylate Copolymerization Based on the Eight AD2 Reactions in Figure 2 over the Temperature Range of 296.15−476.15 K and at 1000 bar and Reactivity Ratios Fitted from Experimental Data at 296.15 K Based on TM by Buback et al.[34] [a]

	r_1		r_2	
T (K)	k_{111}/k_{112}	k_{211}/k_{212}	k_{122}/k_{121}	k_{222}/k_{221}
296.15	6.17	1.99	0.46	1.67
326.15	5.80	1.77	0.51	1.75
356.15	5.50	1.61	0.56	1.83
386.15	5.26	1.49	0.60	1.89
416.15	5.07	1.39	0.64	1.95
446.15	4.91	1.31	0.68	2.00
476.15	4.77	1.24	0.72	2.05
fitted from composition plot	3.03	0.20		
fitted from $k_{p,copo}$ (PLP-SEC)	1.95	0.21		

[a] Kinetic parameters are listed in Table 4, and the pressure adjustment ratios are listed in Table 1.

Table 6. Calculated EPUE Monomer Reactivity Ratios (r_{11}, r_{21}, r_{22}, r_{12}) and Radical Reactivity Ratios (s_1, s_2) for Methyl Methacrylate−Methyl Acrylate Copolymerization Based on the Eight AD2 Reactions in Figure 2 over the Temperature Range of 296.15−476.15 K and at 1000 bar and Reactivity Ratios Fitted from $k_{p,copo}$ at 296.15 K Based on IPUE Model by Buback et al.[34] [a]

T (K)	r_{11} k_{111}/k_{112}	r_{21} k_{211}/k_{212}	r_{22} k_{222}/k_{221}	r_{12} k_{122}/k_{121}	s_1 k_{211}/k_{111}	s_2 k_{122}/k_{222}
296.15	6.17	1.99	1.67	0.46	0.91	0.33
326.15	5.80	1.77	1.75	0.51	0.82	0.32
356.15	5.50	1.61	1.83	0.56	0.75	0.31
386.15	5.26	1.49	1.89	0.60	0.70	0.30
416.15	5.07	1.39	1.95	0.64	0.66	0.29
446.15	4.91	1.31	2.00	0.68	0.63	0.29
476.15	4.77	1.24	2.05	0.72	0.60	0.28
fitted based on IPUE	2.40 (r_1)	0.18 (r_2)	1.46	0.38		

[a] Kinetic parameters are listed in Table 4, and the pressure adjustment ratios are listed in Table 1.

well. For the A-AD3 reactions, at 23 °C and 1000 bar, the calculated monomer reactivity ratios ($r_{11} = 2.50$, $r_{21} = 3.08$, $r_{22} = 0.38$, $r_{12} = 0.38$) and radical reactivity ratios ($s_1 = 2.27$, $s_2 = 0.65$) are in quite good agreement with those fitted based on experiment at 23 °C and 1000 bar: $r_1 = 2.40$, $r_2 = 0.18$, $s_1 = 1.46$, $s_2 = 0.38$. The ratios calculated using the B-AD3 reactions also have values that are consistent with experiment: $r_{11} = 3.11$, $r_{21} = 3.25$, $r_{22} = 0.36$, $r_{12} = 0.38$, $s_1 = 1.15$ and $s_2 = 0.13$.

Overall analysis of the calculated rate coefficients and reactivity ratios based on AD1, AD2, A-AD3, and B-AD3 reactions are consistent with the recommendation put forth previously in our homopolymerization study.[12] AD1 and AD2 capture the general features of the copolymerization reactions; i.e., addition to methyl methacrylate monomer is always favored

Table 7. Activation Energies (E_a), Frequency Factors (A), Heats of Reaction (ΔH_r), and Rate Constants (k_p at 23 °C, 1000 bar) for the Methyl Methacrylate−Methyl Acrylate AD3 Reactions Where Either Methyl Methacrylate (A) or Methyl Acrylate (B) Is the Penpenultimate Unit[a]

reactions		E_a	A	ΔH_r (23 °C)	k_p (23 °C, 1000 bar)
AAA• + A → AAAA•	$k_{A,111}$	22.7	1.55×10^6	−52.3	3.02×10^2
BAA• + A → BAAA•	$k_{B,111}$	22.5	1.82×10^6	−48.5	3.85×10^2
AAA• + B → AAAB•	$k_{A,112}$	25.5	2.14×10^6	−45.7	1.21×10^2
BAA• + B → BAAB•	$k_{B,112}$	25.4	2.10×10^6	−44.3	1.24×10^2
AAB• + A → AABA•	$k_{A,121}$	20.1	5.75×10^6	−65.1	2.90×10^3
BAB• + A → BABA•	$k_{B,121}$	17.4	3.47×10^6	−64.2	5.27×10^3
AAB• + B → AABB•	$k_{A,122}$	23.5	8.91×10^6	−57.5	1.10×10^3
BAB• + B → BABB•	$k_{B,122}$	20.3	4.27×10^6	−54.0	2.00×10^3
ABA• + A → ABAA•	$k_{A,211}$	21.9	2.82×10^6	−50.7	6.88×10^2
BBA• + A → BBAA•	$k_{B,211}$	22.7	2.51×10^6	−53.6	4.43×10^2
ABA• + B → ABAB•	$k_{A,212}$	25.3	3.63×10^6	−45.0	2.24×10^2
BBA• + B → BBAB•	$k_{B,212}$	26.4	3.47×10^6	−50.3	1.36×10^2
ABB• + A → ABBA•	$k_{A,221}$	18.5	4.68×10^6	−80.3	4.51×10^3
BBB• + A → BBBA•	$k_{B,221}$	15.4	1.26×10^7	−87.4	4.31×10^4
ABB• + B → ABBB•	$k_{A,222}$	21.3	6.17×10^6	−70.9	1.69×10^3
BBB• + B → BBBB•	$k_{B,222}$	21.5	6.03×10^7	−72.6	1.56×10^4

[a] Geometry optimization and frequency calculations were performed using UB3LYP/6-31G(d), electronic energies were calculated using MPWB1K/6-31G(d,p), and low frequencies were treated using a one-dimensional internal rotor model: rate coefficients were first calculated at ambient pressure and adjusted to 1000 bar using the ratios listed in Table 1 (k_p: L mol^{-1} s^{-1}, E_a: kJ mol^{-1}, A: L mol^{-1} s^{-1}, ΔH_r: kJ mol^{-1}).

enthalpically as reflected by the lower activation energies and more exothermic heats of reaction, and addition to methyl acrylate is entropically favored as evidenced by the higher frequency factors. However, the monomeric and dimeric radicals are not sufficient to capture the absolute values of the rate coefficients and the reactivity ratios. The chain length dependence of k_p for methyl methacrylate and methyl acrylate homopolymerization based on the harmonic oscillator and hindered rotor models and comparison of these trends to similar studies of other monomers[25,26,37] have been discussed in detail in our earlier paper.[12] Our results in that work and herein promote the use of at least three units for the propagating radical since effects of the long chain need to be captured, and the penpenultimate unit may also have an influence on the rate coefficients. For methyl methacrylate and methyl acrylate, we have shown that the influence of the penpenultimate unit on the activation energy is small, and the EPUE reactivity ratios are affected negligibly. It is also verified that the implicit penultimate model is an accurate description of methyl methacrylate−methyl acrylate copolymerization based on the absolute values of the individual kinetic parameters, as shown by the ratios in Table 9: $k_{A,111}/k_{A,112} \approx k_{A,211}/k_{A,212} \approx k_{B,111}/k_{B,112} \approx k_{B,211}/k_{B,212}$ and $k_{A,222}/k_{A,221} \approx k_{A,122}/k_{A,121} \approx k_{B,222}/k_{B,221} \approx k_{B,122}/k_{B,121}$.

3.3. Prediction of Composition and Overall Rate Coefficient. The next step was to use the calculated values of all the individual rate coefficients to predict additional

Table 8. Calculated TM Reactivity Ratios (r_1, r_2) for Methyl Methacrylate−Methyl Acrylate Copolymerization Based on the 16 AD3 Reactions in Figure 2 over the Temperature Range of 296.15−476.15 K and at 1000 bar and Reactivity Ratios Fitted from Experimental Data at 296.15 K Based on TM by Buback et al.[34] [a]

	r_1 (A-AD3)		r_1 (B-AD3)	
T (K)	$k_{A,111}/k_{A,112}$	$k_{A,211}/k_{A,212}$	$k_{B,111}/k_{B,112}$	$k_{B,211}/k_{B,212}$
296.15	2.50	3.08	3.11	3.25
326.15	2.37	2.71	2.77	2.83
356.15	2.27	2.44	2.51	2.52
386.15	2.19	2.23	2.31	2.29
416.15	2.13	2.07	2.15	2.11
446.15	2.07	1.94	2.03	1.96
476.15	2.02	1.83	1.92	1.84
fitted from composition plot	3.03	3.03		
fitted from $k_{p,copo}$ (PLP-SEC)	1.95	1.95		

	r_2 (A-AD3)		r_2 (B-AD3)	
T (K)	$k_{A,122}/k_{A,121}$	$k_{A,222}/k_{A,221}$	$k_{B,122}/k_{B,121}$	$k_{B,222}/k_{B,221}$
296.15	0.38	0.38	0.38	0.36
326.15	0.43	0.42	0.42	0.46
356.15	0.48	0.46	0.46	0.56
386.15	0.53	0.50	0.50	0.66
416.15	0.57	0.54	0.53	0.76
446.15	0.61	0.57	0.56	0.86
476.15	0.64	0.60	0.59	0.96
fitted from composition plot	0.20	0.20		
fitted from $k_{p,copo}$ (PLP-SEC)	0.21	0.21		

[a] Kinetic parameters are listed in Table 7, and the pressure adjustment ratios are listed in Table 1.

quantities for the different models that are experimentally measured: the composition in the copolymer as a function of the composition of the monomer in the feed and the overall rate coefficient for copolymerization, $k_{p,copo}$. Using the results from the trimeric radicals in which penpenultimate effects were incorporated and averaging the different values listed in Table 9, the two TM reactivity ratios at 23 °C and 1000 bar were obtained:

$$r_1 = 2.99 \qquad r_2 = 0.38$$

Based on averaging the monomer reactivity and radical reactivity ratios for the two different penpenultimate units reported in Table 9, the six EPUE reactivity ratios at 23 °C and 1000 bar were obtained.

$$r_{11} = 2.81 \quad r_{21} = 3.17 \quad r_{22} = 0.37 \quad r_{12} = 0.38$$
$$s_1 = 1.71 \quad s_2 = 0.39$$

Furthermore, the implicit penultimate unit effect model reactivity ratios (r_1 and r_2) were calculated based on further averaging as $r_1 = (r_{11} + r_{21})/2$ and $r_1 = (r_{12} + r_{22})/2$:

$$r_1 = 2.99 \quad r_2 = 0.38 \quad s_1 = 1.71 \quad s_2 = 0.39$$

Thus, there are three different sets of reactivity ratios that can be used to predict the composition and the overall rate coefficient. In the prediction of $k_{p,copo}$, propagation rate coefficients calculated based on AAA$^\bullet$ + A ($k_{A,111} = 3.02 \times 10^2$ L mol^{-1} s^{-1}) and BBB$^\bullet$ + B ($k_{B,222} = 1.56 \times 10^4$ L mol^{-1} s^{-1}) were used for methyl methacrylate and methyl acrylate homopolymerization, respectively.

Using these values, Mayo−Lewis plots of F_{MMA} vs f_{MMA} for methyl methacrylate−methyl acrylate copolymerization at 23 °C and 1000 bar based on the EPUE model (eqs 4 and 5), IPUE model (eq 5), and TM (eq 2) were constructed and are shown in Figure 5. The predicted composition curves are in very good agreement with the experimental data. These three curves for the TM, IPUE, and EPUE models almost overlap, indicating that in the prediction of copolymer composition the simplified TM and IPUE models are good surrogates for the more detailed EPUE model.

With the activation energies and frequency factors for all of the individual reactions in hand, it is interesting to calculate the temperature dependence of the monomer reactivity and radical reactivity ratios of the EPUE model over the range of

Table 9. Calculated EPUE Monomer Reactivity Ratios (r_{11}, r_{21}, r_{22}, r_{12}) and Radical Reactivity Ratios (s_1, s_2) for Methyl Methacrylate−Methyl Acrylate Copolymerization Based on the 16 AD3 Reactions in Figure 2 over the Temperature Range of 296.15−476.15 K and at 1000 bar and Reactivity Ratios fitted from $k_{p,copo}$ at 296.15 K Based on IPUE Model by Buback et al.[34] [a]

T (K)	r_{11} $k_{A,111}/k_{A,112}$	r_{21} $k_{A,211}/k_{A,212}$	r_{22} $k_{A,222}/k_{A,221}$	r_{12} $k_{A,122}/k_{A,121}$	s_1 $k_{A,211}/k_{A,111}$	s_2 $k_{A,122}/k_{A,222}$
296.15	2.50	3.08	0.38	0.38	2.27	0.65
326.15	2.37	2.71	0.42	0.43	2.09	0.70
356.15	2.27	2.44	0.46	0.48	1.95	0.74
386.15	2.19	2.23	0.50	0.53	1.84	0.78
416.15	2.13	2.07	0.54	0.57	1.75	0.82
446.15	2.07	1.94	0.57	0.61	1.68	0.85
476.15	2.02	1.83	0.60	0.64	1.62	0.88
fitted	2.40 (r_1)	0.18 (r_2)	1.46	0.38		

T (K)	r_{11} $k_{B,111}/k_{B,112}$	r_{21} $k_{B,211}/k_{B,212}$	r_{22} $k_{B,222}/k_{B,221}$	r_{12} $k_{B,122}/k_{B,121}$	s_1 $k_{B,211}/k_{B,111}$	s_2 $k_{B,122}/k_{B,222}$
296.15	3.11	3.25	0.36	0.38	1.15	0.13
326.15	2.77	2.83	0.46	0.42	1.17	0.12
356.15	2.51	2.52	0.56	0.46	1.18	0.12
386.15	2.31	2.29	0.66	0.50	1.20	0.11
416.15	2.15	2.11	0.76	0.53	1.21	0.11
446.15	2.03	1.96	0.86	0.56	1.22	0.10
476.15	1.92	1.84	0.96	0.59	1.23	0.10
fitted	2.40(r_1)	0.18(r_2)	1.46	0.38		

[a] Kinetic parameters are listed in Table 7, and the pressure adjustment ratios are listed in Table 1.

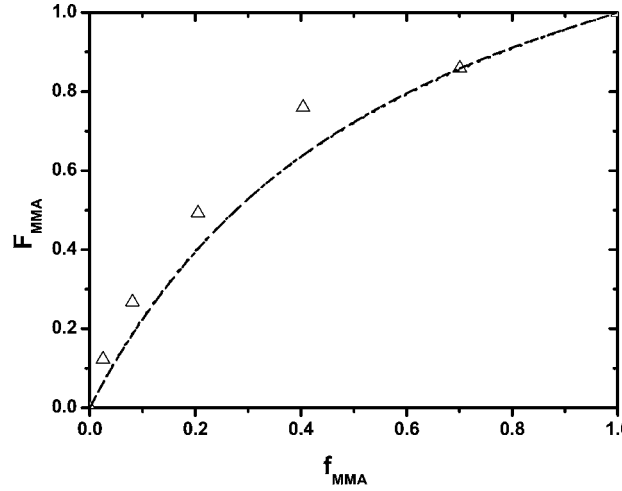

Figure 5. Mayo−Lewis plot for methyl methacrylate (MMA)−methyl acrylate copolymerization at 23 °C and 1000 bar: experimental data (triangles), terminal model (dashed line r_1 and r_2 are the average values of the data listed in Table 8: $r_1 = 2.99$, $r_2 = 0.38$), explicit penultimate effect model (dotted line, r_{ij} and s_i are average values of the data listed in Table 9: $r_{11} = 2.81$, $r_{21} = 3.17$, $r_{12} = 0.38$, $r_{22} = 0.37$), implicit penultimate effect model (dashed-dotted line, r_j values are the average of EPUE r_{ij}: $r_1 = 2.99$, $r_2 = 0.38$).

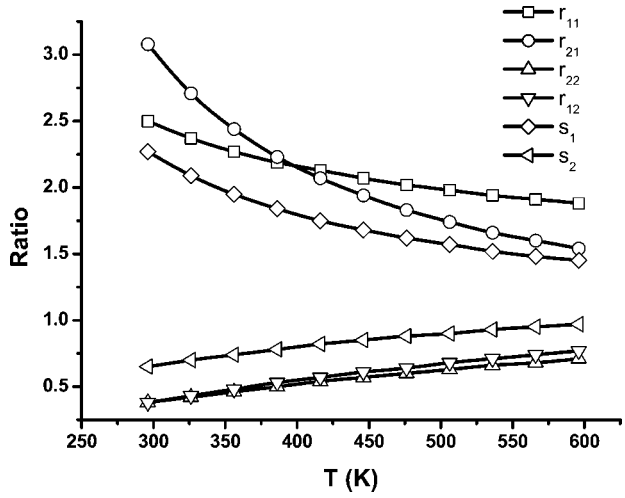

Figure 6. Change in the monomer reactivity and radical reactivity ratios characterizing the EPUE model with temperature over the range of 296.15−596.15 K at 1000 bar. The activation energies and frequency factors are from the A-AD3 reactions as listed in Table 7.

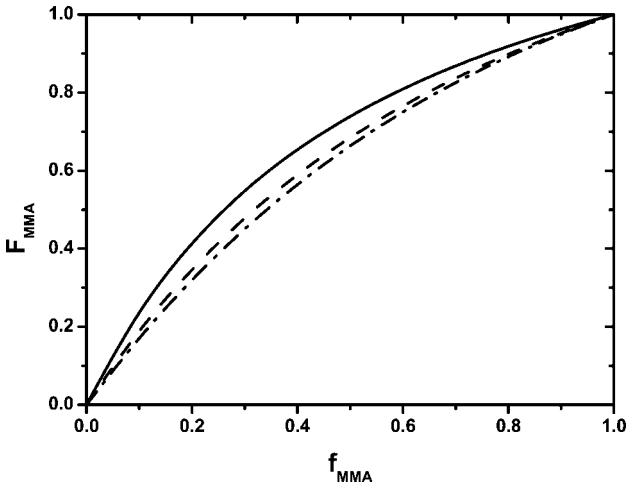

Figure 7. Mayo−Lewis plots for methyl methacrylate (MMA)−methyl acrylate copolymerization at three temperatures: 296.15 K (solid line), 373.15 K (dashed line), and 423.15 K (dashed-dotted line); 1000 bar based on the EPUE model. The activation energies and frequency factors are from the A-AD3 reactions in Table 7.

296.15−596.15 K at 1000 bar. These values are calculated based on the activation energies and frequency factors from the A-AD3 reactions and are plotted in Figure 6. As expected, the values are all approaching a value of 1.0 at high temperature, but this plot nicely illustrates the rate at which this high-temperature asymptote is reached. It is more interesting to see what impact these changes have on the copolymer composition as a function of temperature. The predicted compositions at temperatures of 296.15, 373.15, and 423.15 K are shown in Figure 7. With increasing temperature, the curves are approaching the line of parity, which means the preference of the radicals to react with methyl methacrylate is becoming less significant. This example illustrates how ab initio calculations can be used to predict the topology of copolymers.

The predicted values of the overall rate constants ($k_{p,copo}$) as a function of the monomer fraction calculated with the TM, IPUE, and EPUE models are shown in Figure 8. The results are generally in agreement with the experimental values. The deviation is because the calculated value for k_p of methyl methacrylate homopolymerization is about a factor of 2 too low, which is most pronounced as the mixture becomes more rich in methyl methacrylate. The calculated value for k_p of methyl

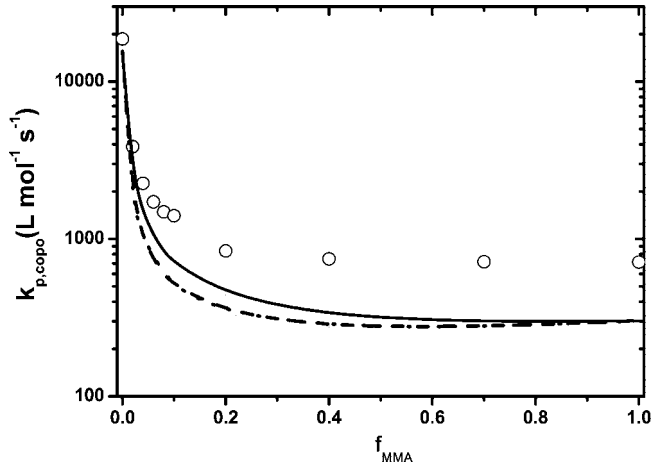

Figure 8. Propagation rate constant $k_{p,copo}$ for methyl methacrylate (MMA)−methyl acrylate copolymerization at 23 °C and 1000 bar: PLP-SEC data (circles), explicit penultimate effect model prediction (solid line), implicit penultimate effect model prediction (dotted line), and terminal model prediction (dashed line), $k_{p,MMA}$ and $k_{p,MA}$ were calculated using AAA$^\bullet$ + A (3.02×10^2 L mol^{-1} s^{-1}) and BBB$^\bullet$ + B (1.56×10^4 L mol^{-1} s^{-1}), respectively; the reactivity ratios for TM: $r_1 = 2.99$, $r_2 = 0.38$; the monomer reactivity and radical reactivity ratios for EPUE: $r_{11} = 2.81$, $r_{21} = 3.17$, $r_{22} = 0.37$, $r_{12} = 0.38$, $s_1 = 1.71$, and $s_2 = 0.39$; the monomer reactivity and radical reactivity ratios for IPUE: $r_1 = 2.99$, $r_2 = 0.38$, $s_1 = 1.71$, and $s_2 = 0.39$.

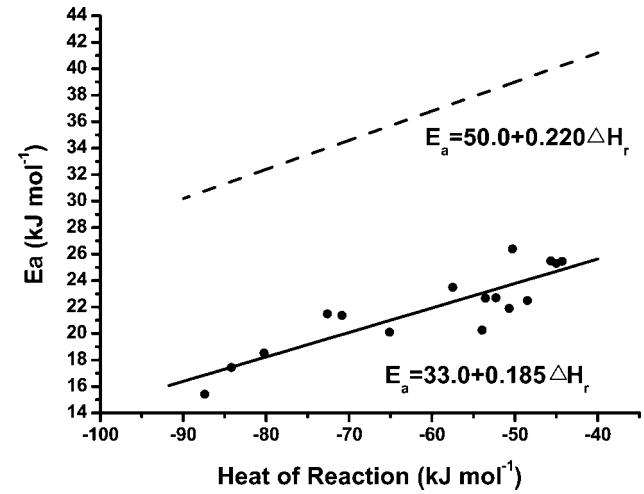

Figure 9. Activation energy (E_a) as a function of heat of reaction (ΔH_r) for the 16 AD3 reactions summarized in Table 7 (circles); the linear relationship regressed (solid line) is $E_a = 33.0 + 0.185\Delta H_r$, $R^2 = 0.77$; the dashed line is the upper limiting correlation between E_a and ΔH_r for radical addition to alkenes presented by Fischer and Radom.[13]

acrylate is in better quantitative agreement with the experimental value, which results in the predicted $k_{p,copo}$ matching very well at low methyl methacrylate fractions. The predicted rate coefficients using the TM are very close to those predicted using the IPUE model, as can be seen from the plot. However, these results are distinctly different from the values calculated using the EPUE model in the intermediate f_{MMA} region, which are closer to the experimental data. Thus, while the penultimate model is not differentiated by the composition values, the effect of the penultimate unit does manifest itself to a small but measurable extent in $k_{p,copo}$.

3.4. Correlation Between E_a and ΔH_r. Finally, the relationship between the activation energy (E_a) and the heat of reaction (ΔH_r) was also investigated based on the 16 AD3 reactions as shown in the plot in Figure 9. A linear relationship that is consistent with the Evans−Polanyi relationship is apparent:

$$E_a = 33.0 + 0.185\Delta H_r \quad (16)$$

with a relatively good regression coefficient (R^2 equals 0.77). An upper limiting correlation between E_a and ΔH_r for radical addition to alkenes was provided by Fischer and Radom and is shown as eq 17:[13]

$$E_a = 50.0 + 0.220\Delta H_r \quad (17)$$

which is plotted as the dashed line in Figure 9. The upper limiting correlation represents the dependence on enthalpy alone; i.e., polar and steric effects can be neglected. The relationship regressed based on the 16 AD3 reactions has a less pronounced slope, which is consistent with electrophilic polar effects. The regressed E_0 value is about 17 kJ mol^{-1} lower than the upper limit, which is consistent with Fischer and Radom's observations that polar effects lower the activation energy.

4. Conclusion

Methyl methacrylate and methyl acrylate copolymerization reactions were studied using addition of monomeric, dimeric, and trimeric radicals to monomers using quantum chemistry and transition state theory. The use of radicals of different length allowed penultimate and penpenultimate effects to be explored and different models of copolymerization (TM, EPUE, and IPUE) to be tested. Unrestricted B3LYP/6-31G(d) was used for geometry optimization and potential energy scans, and the electronic energies were calculated using MPWB1K/6-31G(d,p). Low frequencies were treated using a one-dimensional internal rotor model in the calculation of partition functions for rate constants and thermodynamic properties. It was found that addition reactions involving monomeric or dimeric radicals offered results that were qualitatively consistent with experimental data, but quantitatively accurate monomer and radical reactivity ratios and rate coefficients were not obtained. However, rate coefficients and monomer and radical reactivity ratios for the TM and PUE models which were in good agreement with those fitted from experimental data were obtained when the radical chain length was three. Although the penpenultimate unit had a negligible influence on the activation energy values, its entropic influence was reflected in the frequency factor and thus the rate coefficient. The predicted copolymer compositions using the TM, IPUE, and EPUE models are very close to one another, while the predicted overall rate coefficient ($k_{p,copo}$) based on the EPUE model had a measurable difference from those based on the TM and IPUE models. Finally, the relationship between the activation energy and the reaction enthalpy based on the 16 AD3 reactions was examined, and the Evans−Polanyi relationship was shown to be obeyed.

Acknowledgment. We gratefully acknowledge the Inter-American Materials Collaboration Program of the National Science Foundation (DMR-0303435), the MRSEC program of the National Science Foundation (DMR-0076097), and the US−Israel Binational Science Foundation (Grant #2002408) for financial support. Funding was also provided through the National Science Foundation Graduate Fellowship Program (Seth E. Levine). Supercomputer resources from NCSA (TG-CTS050021N) are also acknowledged.

References and Notes

(1) Meyer, T.; Keurentjes, J. *Handbook of Polymer Reaction Engineering*, 1st ed.; Wiley-VCH: New York, 2005.
(2) Beuermann, S.; Buback, M. *Prog. Polym. Sci.* **2002**, *27*, 191.
(3) Hutchinson, R. A.; John, H. M.; Donald, A. P. *Ind. Eng. Chem. Res.* **1997**, *36*, 1103.
(4) Kululj, D.; Davis, T. *Macromolecules* **1998**, *31*, 5668.
(5) Coote, M. L.; Davis, T. P. *Prog. Polym. Sci.* **1999**, *24*, 1217.
(6) Buback, M.; Feldermann, A.; Barner, C. K. *Macromolecules* **2001**, *34*, 5439.
(7) Coote, M. L.; Michael, D. Z.; Davis, T. P.; Willett, G. D. *Macromolecules* **1997**, *30*, 8182.
(8) Coote, M. L.; Johnston, L. P.; Davis, T. *Macromolecules* **1997**, *30*, 8191.
(9) Fukuda, T.; Ma, Y.-D.; Inagaki, H. *Macromolecules* **1985**, *18*, 17.
(10) Beuermann, S.; Paquet, J.; McMinn, J. *Macromolecules* **1996**, *29*, 4206.
(11) Buback, M.; Kurz, C.; Schmaltz, C. *Macromol. Chem. Phys.* **1998**, *199*, 1721.
(12) Yu, X.; Pfaendtner, J.; Broadbelt, L. J. *J. Phys. Chem. A* **2008**, *112*, 6772.
(13) Fischer, H.; Radom, L. *Angew. Chem., Int. Ed.* **2001**, *40*, 1340.
(14) Pfaendtner, J.; Yu, X.; Broadbelt, L. J. *J. Phys. Chem. A* **2006**, *110*, 10863.
(15) Wong, M. W.; Pross, A.; Radom, L. *J. Am. Chem. Soc.* **1994**, *116*, 11938.
(16) Gomez-Balderas, R.; Coote, M. L.; Henry, D. J.; Fischer, H.; Radom, L. *J. Phys. Chem. A* **2003**, *107*, 6082.
(17) Shaik, S. S.; Canadell, E. *J. Am. Chem. Soc.* **1990**, *112*, 1446.
(18) Frisch, M. J.; Trucks, G. W.; Schlegel, H. B.; Scuseria, G. E.; Robb, M. A.; Cheeseman, J. R.; Montgomery, J. A.; Vreven, J. T.; Kudin, K. N.; Burant, J. C.; Millam, J. M.; Iyengar, S. S.; Tomasi, J.; Barone, V.; Mennucci, B.; Cossi, M.; Scalmani, G.; Rega, N.; Petersson, G. A.; Nakatsuji, H.; Hada, M.; Ehara, M.; Toyota, K.; Fukuda, R.; Hasegawa, J.; Ishida, M.; Nakajima, T.; Honda, Y., Kitao, O.; Nakai, H.; Klene, M.; Li, X.; Knox, J. E.; Hratchian, H. P.; Cross, J. B.; Adamo, C.; Jaramillo, J.; Gomperts, R.; Stratmann, R. E.; Yazyev, O.; Austin, A. J., Cammi, R.; Pomelli, C.; Ochterski, J. W.; Ayala, P. Y.; Morokuma, K.; Voth, G. A.; Salvador, P.; Dannenberg, J. J.; Zakrzewski, V. G.; Dapprich, S.; Daniels, A. D.; Strain, M. C.; Farkas, O.; Malick, D. K.; Rabuck, A. D.; Raghavachari, K.; Foresman, J. B.; Ortiz, J. V.; Cui, Q.; Baboul, A. G.; Clifford, S.; Cioslowski, J.; Stefanov, B. B.; Liu, G.; Liashenko, A.; Piskorz, P.; Komaromi, I.; Martin, R. L.; Fox, D. J.; Keith, T.; Al-Laham, M. A.; Peng, C. Y.; Nanayakkara, A.; Challacombe, M.; Gill, P. M. W.; Johnson, B.; Chen, W.; Wong, M. W.; Gonzalez, C.; Pople, J. A. Gaussian 03, revision c.02 edition, Gaussian, Inc., Wallingford, CT, 2004.
(19) Foresman, J. B. *Exploring Chemistry with Electronic Structure Methods*, 1st ed.; Gaussian Inc.: Pittsburgh, PA, 2002.
(20) Pfaendtner, J.; Yu, X.; Broadbelt, L. J. *Theor. Chem. Acc.* **2007**, *118*, 881.
(21) *Gaussian 03 Manual*, 1st ed.; Gaussian Inc.: Pittsburgh, PA, 1990.
(22) Scott, A. P.; Radom, L. *J. Phys. Chem.* **1996**, *100*, 16502.
(23) McQuarrie, D. A.; Simon, J. D. *Molecular Thermodynamics*, 1st ed.; University Science Books: Sausalito, CA, 1999.
(24) Heuts, J. P.; Gilbert, R. G. *Macromolecules* **1995**, *28*, 8771.
(25) Izgorodina, E. I.; Coote, M. L. *Chem. Phys.* **2006**, *324*, 96.
(26) Van Cauter, K.; Van Speybroeck, V.; Vansteenkiste, P.; Reyniers, M. F.; Waroquier, M. *ChemPhysChem* **2006**, *7*, 131.
(27) Van Speybroeck, V.; Van Neck, D.; Waroquier, M.; Wauters, S.; Saeys, M.; Martin, G. B. *J. Phys. Chem. A* **2001**, *105*, 7713.
(28) Huang, M. D.; Monteiro, J. M.; Gilbert, R. G. *Macromolecules* **1998**, *31*, 5175.
(29) Sumathi, R.; Carstensen, H.; Green, W. H. *J. Phys. Chem.* **2001**, *105*, 6910.
(30) Van Speybroeck, V.; Van Neck, D.; Waroquier, M. *J. Phys. Chem. A* **2002**, *106*, 8945.
(31) Van Speybroeck, V.; Vansteenkiste, P.; Van Neck, D.; Waroquier, M. *Chem. Phys. Lett.* **2005**, *402*, 479.
(32) East, A. L. L.; Radom, L. *J. Phys. Chem.* **1997**, *106*, 6655.
(33) Balint-Kurti, G. G.; Dixon, R. N.; Marston, C. C. *Int. Rev. Phys. Chem.* **1992**, *11*, 317.
(34) Buback, M.; Müller, E. *Macromol. Chem. Phys.* **2007**, *208*, 581.
(35) Odian, G. *Principles of Polymerization*, 4th ed.; Wiley-Interscience: New York, 2004.
(36) Beuermann, S.; Buback, M.; Russell, G. T. *Macromol. Rapid Commun.* **1994**, *15*, 351.
(37) Heuts, J. P.; Russell, G. T. *Eur. Polym. J.* **2006**, *42*, 3.

MA801241P